

The ATLAS Liquid Argon Calorimeter at the LHC

Iro Koletsou, LAPP, CNRS/IN2P3, Annecy-le-vieux
on behalf of the ATLAS Liquid Argon Calorimeter Group

Abstract

The Liquid Argon (LAr) calorimeter is a key detector component in the ATLAS experiment at the LHC. It has been installed in the ATLAS cavern and is filled with liquid argon since 2006. Its performance has been studied using random triggers, calibration data, cosmic muons (from September-October 2008 and June-July 2009 cosmic data taking), LHC beam splash events (from September 2008 and November 2009 LHC running), and collision events (from November and December 2009 LHC running). The properties of each read-out channel such as pedestal, noise and gain have been measured and the high stability of the LAr electronics over several months of data taking is shown. Calibration data are stored into a database and used at reconstruction level (online and offline). The quality of the energy reconstruction at the first trigger level has also been studied. The method used to predict the ionization pulse shape is presented and the prediction is compared to ionization signals from cosmic muons. The uniformity of the calorimeter response has also been measured. Splash events have been used to estimate the calorimeter timing. Moreover, the missing transverse energy resolution has been evaluated using collision events and compared to the expected resolution.

Key words: LHC, ATLAS, Liquid Argon Calorimeter

1. Introduction

The Liquid Argon (LAr) sampling calorimeter is a fundamental piece of the ATLAS detector. The achievement of the most important goals of the ATLAS experiment, such as the search for the Higgs boson and for signatures of supersymmetric particles, depends on its performance and the excellent functionality of each of its components. There are three components of the ATLAS LAr calorimeters: the electromagnetic (EM) barrel and endcaps, the hadronic endcap and the forward calorimeter.

The EM calorimeter (barrel and endcaps) covers the pseudorapidity (defined as $\eta = -\ln \tan(\theta/2)$) range of $0 < |\eta| < 3.2$ and uses lead absorbers. It is built in an accordion shape which provides a hermetic coverage in ϕ . It is separated into three longitudinal layers, the first from the centre has an excellent granularity: $\Delta\eta \times \Delta\phi = 0.003 \times 0.1$ for $|\eta| < 1.8$ (excluding the transition region between barrel and endcaps). For $|\eta| < 1.8$ a pre-sampler is placed in front of the first layer and is used to estimate the energy losses due to the material in front of the calorimeter. The energy resolution is $\sigma(E)/E \sim 10\% / \sqrt{E} \oplus 0.7\%$.

The hadronic endcap covers the pseudorapidity range of $1.5 < |\eta| < 3.2$. It is separated into four longitudinal layers and uses copper as the absorber. The energy resolution is given by $\sigma(E)/E \sim 50\% / \sqrt{E} \oplus 3\%$. In the barrel region, the hadronic calorimetry is performed with an iron-scintillator tile calorimeter.

The forward calorimeter covers the high pseudorapidity regions: $3.1 < |\eta| < 4.9$. It has one electromagnetic layer with copper as passive material and two hadronic layers which are using tungsten absorbers. The hadronic energy resolution is $\sigma(E)/E \sim 100\% / \sqrt{E} \oplus 10\%$.

The three subdetectors are positioned in three cryostats that are filled with liquid argon which acts as active medium. The three subdetectors share the same read-out electronics. In total there are 182468 channels that can be calibrated individually. The readout is functional for 98.6% of the cells. The remaining 1.4% of the cells are not read out because they are connected to 18 non-functioning Front End Boards (FEB). In these FEBs, it is the active part (VCSEL) of the optical transmitter to the ROD that has failed. The causes of this failures, that occurred with a rate of two or three devices per month, is under investigation. This problem will be fixed during the next LHC shutdown. Another 0.05% of the cells are masked in the event reconstruction because they are either not responding to the input pulse (0.02%) or they are permanently noisy (0.03%). In total, 1.3% of the cells are not used in the event reconstruction; but this number is expected to decrease in a very significant way during the next LHC shutdown.

2. Electronic calibration and energy reconstruction

The principle of detection is the generation of a shower in the absorber and then the ionization of the liquid argon. The ionization electrons drift to the anodes under the high voltage (HV) which is of the order of 1 kV/mm. The amplitude of the resulting triangular signal is proportional to the deposited energy. The signal is then pre-amplified and shaped in the Front End Boards placed around the liquid argon cryostats, and then sampled around the pulse maximum: typically five amplitude measurements are taken, spaced by 25 ns. The maximum am-

plitude A_{max} is computed as follows:

$$A_{max} = \sum_{j=1}^{N_{samples}} a_j (s_j - p) \quad (1)$$

where a_j are the Optimal Filtering Coefficients [1], p the pedestal, and s_j the amplitudes of the $N_{samples}$ samples. The reconstructed cell energy E_{cell} is then:

$$E_{cell} = F_{\mu A \rightarrow MeV} \cdot F_{DAC \rightarrow \mu A} \cdot \frac{1}{\frac{M_{phys}}{M_{cali}}} \cdot R \cdot A_{max} \quad (2)$$

where R is the factor which transforms ADC into DAC values (called gain in the following). The conversion factor $F_{\mu A \rightarrow MeV}$ depends on the sampling fraction, is estimated with Geant 4 simulations, and results from test beams. The conversion factor $F_{DAC \rightarrow \mu A}$ takes into account calibration board specificities. $\frac{M_{phys}}{M_{cali}}$ describes the difference in maximum amplitude between an ionization and a calibration signal. The values of p , of a_j , and of R are computed using dedicated calibration runs and their stability is crucial to ensure the required energy resolution. In Fig. 1 the stability of the gain (R) is shown over time. The level of stability between two consecutive runs is better than 0.1%. The shifts of the gain observed in some runs are due to the unstable conditions during the calibration runs and are expected to vanish with the collision stable runs. The effect is in any case corrected by the frequent update of the data base.

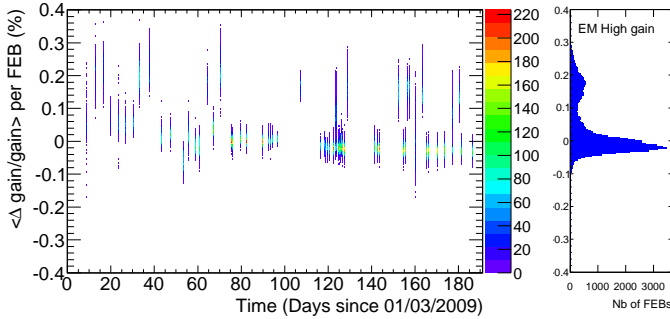


Figure 1: Stability of the gain (R) over time. The deviations between two runs are smaller than 0.1%.

3. Commissioning with cosmic muons

In 2008, the installation of the detectors in the ATLAS cavern was completed. Since then, a significant effort has been dedicated to the analysis of data taken from cosmic rays. Radiative cosmic muons are used to test the quality of the prediction of an ionization signal shape by the calibration procedure. Their signals are recorded with 32 samples in order to study the complete pulse shape. Fig. 2 shows the difference between a predicted signal shape and a real ionization signal in the second layer of the EM barrel, induced by a cosmic muon. The prediction is of very high quality, the residuals being smaller than 2%. Similar agreement is obtained for every layer in every subdetector.

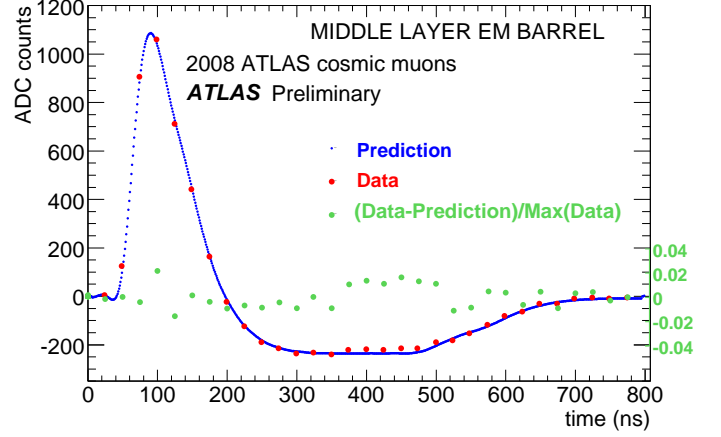


Figure 2: A typical pulse in the second layer of the EM barrel calorimeter. The dense sequence of small dots corresponds to the prediction, the bigger dark dots indicate the data, and the lighter points correspond to the difference in percentage between data and prediction (right scale).

Cosmic muons were also an excellent tool for the measurement of the uniformity of response. Muons are reconstructed by using events with a projective track in the tracking detector (located inside of the LAr barrel cryostat) and following an iterative procedure to select the best phase for the sampling and the energy reconstruction, as cosmic events are asynchronous with respect to the sampling command. The uniformity is defined as the relative variation of the data with respect to the prediction. More precisely, a binning in η (optimised according to the available statistics) is performed and then a Landau convoluted with a gaussian distribution is used to fit the muon's energy in every bin. The most probable value of the Landau curve for the data is then compared to the Monte Carlo result. As seen in Fig. 3 for the middle layer of the EM barrel, the non-uniformity is 1.2%. It is 1.7% for the front layer [3].

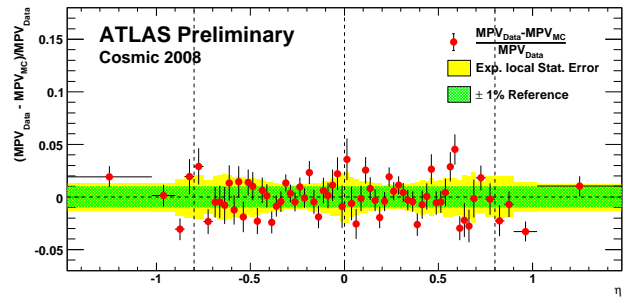


Figure 3: Normalized residual of the most probable value (MPV) from data and prediction. The constant band at ± 0.01 represents a reference of an agreement to 1%. The light coloured band represents the expected local statistical error for that region.

In Fig. 2 the undershoot of the pulse can also be clearly seen. Its length is related to the drift time of ionization electrons and the rising at the end of the pulse is sensitive to a dispersion of the gaps over the charge collection area. The drift time non-uniformity is a very important parameter to study, as it has a

non-negligible contribution to the constant term of the energy resolution. Fig. 4 shows the drift time in the EM LAr calorimeter. It is almost constant in the barrel, because of the constant gap size and the constant HV, and very varying in the endcaps, where the size of the gap depends on the pseudorapidity η . The non-uniformities of the gap size are estimated to have a contribution to the constant term of the energy resolution of 0.29% in the barrel, and of 0.53% in the endcaps [2, 3].

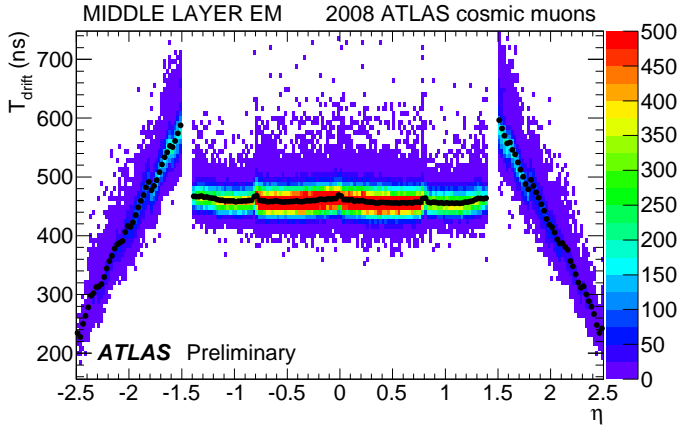


Figure 4: Drift time on the middle layer of the EM calorimeter as a function of η . The gap size decreasing with $|\eta|$ is reflected in the EM endcaps while it is constant in the EM barrel.

4. Commissioning with splash events

In October 2008 and November 2009, a single beam circulated in the LHC tunnel. It was then possible to see “splash events” by using closed collimators located 200 m ahead of the interaction point. Muons and pions from this interaction reached ATLAS and produced a significant activity in the detector, including the LAr calorimeters. Using these splash events, a timing alignment of the detector is possible. This can be done as follows: the time of the maximum amplitude of the ionization signal is identified by an iterative procedure. More precisely, this is done by iterating on the event phase until the time determined by the optimal filtering is smaller than the time interval between two OFC (Optimal Filtering Coefficients) sets. Then, a time-of-flight correction is applied (with respect to the collision configuration), assuming a flux of particles parallel to the beam axis. Finally, the relative time is calculated for every FEB of the electromagnetic barrel. The average time among the 128 channels of each FEB is computed, and the reference is defined as the average time measured for FEBs from the region $|\eta| < 0.4$. As can be seen in Fig. 5, taken as example for every subdetector, the time accuracy is measured to be of the order of 1 ns.

5. Commissioning with collisions

The ATLAS experiment has recorded LHC collision events in November and December 2009, at a centre-of-mass energy

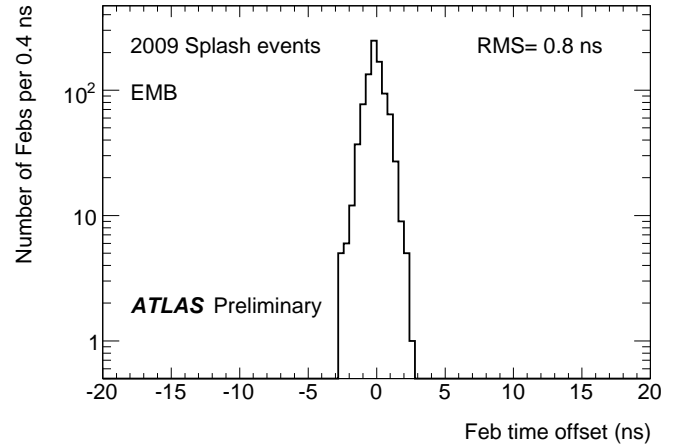


Figure 5: Distribution of the relative time for every FEB of the electromagnetic barrel calorimeter.

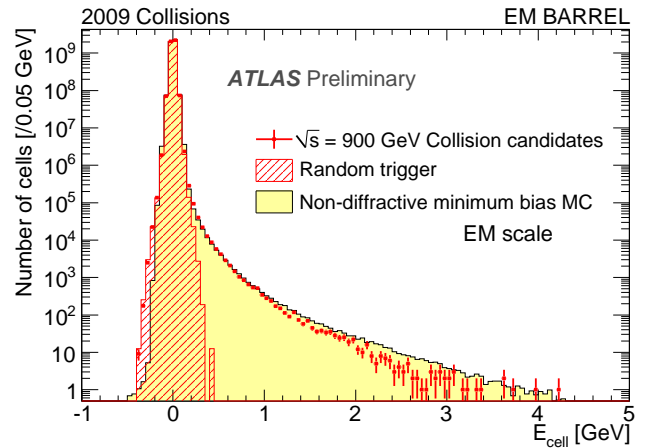


Figure 6: Distribution of the cell energy with collision events for the EM barrel. The cell energy distribution from random data (contribution of electronic noise only) is also shown, as well as non-diffractive minimum bias Monte Carlo events. All cells, but the ones known to be noisy and which are masked, are entered in the distributions.

of 900 GeV, and of 2.36 TeV. In Fig. 6 we can see the energy in the EM barrel cells for a random trigger (without collisions, hatched histogram) and for 900 GeV collision data (histogram for the Monte Carlo, crosses for the collision candidates). The predicted energy deposition is very close to the measured one; we can clearly see the difference between the random trigger case and the collision data.

The 900 GeV and 2.36 TeV runs were used to make an estimation of the missing transverse energy (E_T) resolution. To compute the missing E_T the complete calorimeter range has been used and only cells belonging to reconstructed clusters have been considered, to reduce the effect of the noise. Fig. 7 shows the resolution of the x and y components of the missing E_T as a function of the overall transverse energy in the complete calorimeter range, as predicted by Monte Carlo and as measured with the 900 GeV and the 2.36 TeV data. The data are very close to the prediction and the results can be further

improved by using a dedicated calibration for every final state object (such as electrons, photons, jets) and a hadronic calibration.

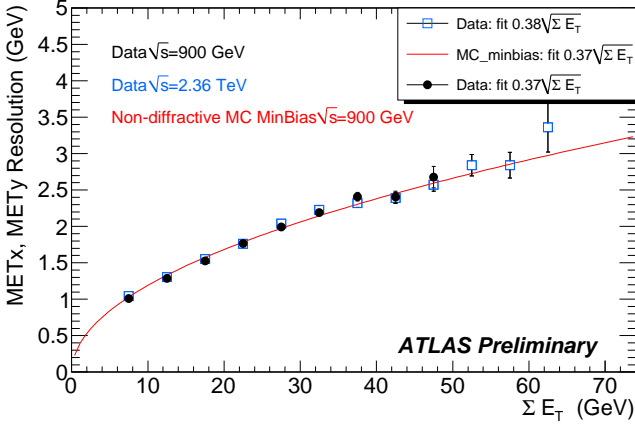


Figure 7: Resolution of the two components of the missing transverse energy as a function of the total sum of the transverse energy, at a centre-of-mass energy of 2.36 TeV (open squares), and of 900 GeV (filled circles). The line shows a fit to the Monte Carlo simulation.

A very significant effort has also been dedicated to trigger studies. In the first level of the trigger, the first online energy computation is performed. The energy is measured using trigger towers with a size of $\Delta\eta \times \Delta\phi = 0.1 \times 0.1$. Fig. 8 shows the correlation between the trigger online energy and the offline reconstructed energy. The transverse energy resolution of the Level-1 trigger with respect to the reconstructed E_T is better than 5% for objects with $E > 10 \text{ GeV}$.

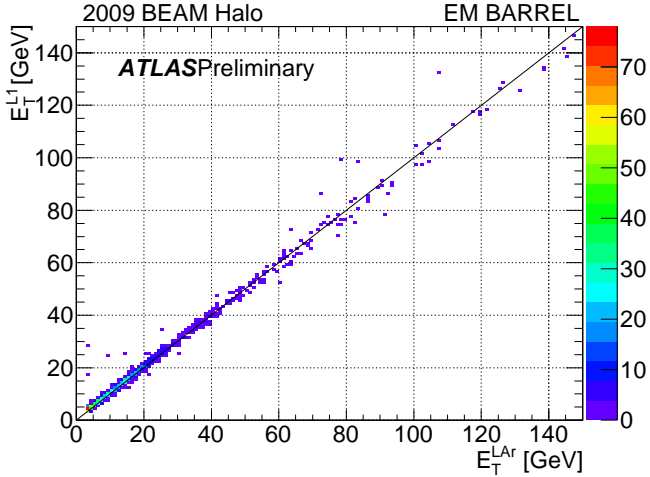


Figure 8: Correlation between the online computation of the Level 1 trigger and the offline reconstructed energy.

6. Conclusions

The ATLAS Liquid Argon calorimeter is completely installed in the ATLAS cavern since 2008. The commission-

ing and calibration campaigns have been continuous and crucial for its performance. They have taken place using calibration runs, test beam analysis, cosmic muon data taking, splash events from the September 2008 and November 2009 LHC single beam, and finally proton-proton collisions. It has been shown that the performance of the Liquid Argon calorimeter is excellent and very close to the expectations.

References

- [1] "Signal processing consideration for liquid ionization calorimeters in a high rate environment", W.E. Cleland, E.G. Stern, Nucl. Instr. and Meth. A 338 (1994) 467.
- [2] "Drift Time Measurement in the Atlas Liquid Argon Electromagnetic Calorimeter using Cosmic Muons", The ATLAS Collaboration, arXiv:1002.4189, submitted to EPJC (22 Feb 2010).
- [3] "Readiness of liquid argon calorimeter for LHC collisions", The ATLAS Collaboration, arXiv:0912.2642, submitted to EPJC (14 Dec 2009).